

Atomki anomaly and dark matter in a radiative seesaw model with gauged $B - L$ symmetry

Osamu Seto^{1,2,*} and Takashi Shimomura^{3,†}

¹*Institute for International Collaboration,
Hokkaido University, Sapporo 060-0815, Japan*

²*Department of Physics, Hokkaido University, Sapporo 060-0810, Japan*

³*Faculty of Education, Miyazaki University, Miyazaki, 889-2192, Japan*

(Dated: October 26, 2021)

Abstract

Motivated by recently reported anomalies in a decay of an excited state of beryllium by the Atomki Collaboration, we study a radiative seesaw model with gauged $B - L$ symmetry and a Z_2 parity. Assuming that the anomalies originate from the decay of the $B - L$ gauge boson followed by the nuclear decay, the mass of the lightest right-handed neutrino or the dark matter candidate can be determined below 10 GeV. We show that for this mass range, the model can explain the anomalies in the beryllium decay and the relic dark matter abundance consistent with neutrino masses. We also predict its spin-independent cross section in direct detection experiments for this mass range.

Keywords:

*Electronic address: seto@particle.sci.hokudai.ac.jp

†Electronic address: shimomura@cc.miyazaki-u.ac.jp

I. INTRODUCTION

The Standard Model (SM) of particle physics has been explaining almost all of experimental results including recent LHC data. Despite its enormous success, some phenomena are left unexplained in the SM. One of such phenomena is neutrino oscillations, which result in nonzero and tiny neutrino masses as well as flavor mixing. Another one is the existence of dark matter (DM). Since neutrinos are massless and no candidates exist in the SM, these phenomena are clear evidences of new physics beyond the SM.

Several mechanisms have been proposed to explain the tininess of neutrino mass. The most popular mechanism is the so-called type I seesaw mechanism [1–4]. In the mechanism, right-handed (RH) neutrinos with heavy Majorana masses are introduced to the SM, and the tiny neutrino masses can be explained by a suppression of their heavy mass. There are other types of seesaw mechanisms, type II [5–7], type III [8] and radiative models [9–11]. In radiative seesaw mechanisms, a discrete parity is generally imposed to the SM so that neutrinos can not have tree-level masses or Yukawa interactions (For pioneering works, see e.g. Refs [12, 13]). Then, neutrino masses are generated at loop-level in which new scalars and/or fermions propagate. The masses generated are suppressed by the masses of the new particles in the loop and a loop factor. Tininess of neutrino masses is explained in this sense. In addition to the generation of neutrino mass, the radiative seesaw mechanisms have another virtue. The lightest particle with odd parity becomes stable due to the discrete parity. Such a stable particle can be a good candidate for the DM. In fact, many radiative seesaw models can predict the correct DM abundance. Thus, the two phenomena mentioned above can be explained simultaneously.

Recently, the Atomki Collaboration has reported anomalies in the distributions of the invariant mass and the opening angle of an emitted electron-positron pair from the decay of an excited state of beryllium (^8Be) into its ground state [14]. They claimed that the deviation from a standard nuclear physics interpretation reaches to 6.8σ , and hence, the deviation is probably not a nuclear physics origin. We refer these anomalies to the Atomki anomalies. One of the possibilities to explain the anomalies is the subsequent decay of an unknown particle produced in the ^8Be decay. The Atomki Collaboration assumed a new boson particle with spin-parity $J^\pi = 1^+$ and determined its mass as $m = 16.70 \pm 0.35(\text{stat}) \pm 0.5(\text{syst})$ MeV from their data. It is natural to consider that the boson acquires such a light mass from a spontaneous breakdown of a symmetry. Then, a fundamental scale of the nature can be determined. In [15, 16], the authors showed the Atomki anomalies can be explained by a gauge boson in classes of models with gauged *baryon* (B) and *baryon minus lepton* ($B - L$) symmetry. These gauge symmetries are one of the minimal extensions of the SM, and have been extensively studied in terms of various motivations. There are also studies to explain the Atomki anomalies in other gauge symmetries [17, 18], with an axial vector [19] and pseudoscalars [20]. Implications on the DM have also been studied [21–23].

In this paper, we study the implications of the Atomki anomalies in a radiative seesaw

| | Q^i | d_R^i | u_R^i | L^i | e_R^i | Φ | η | S | N_R^α |
|--------------|-------|---------|---------|-------|---------|--------|--------|-----|--------------|
| $SU(3)_C$ | 3 | 3 | 3 | 1 | 1 | 1 | 1 | 1 | 1 |
| $SU(2)_W$ | 2 | 1 | 1 | 2 | 1 | 2 | 2 | 1 | 1 |
| $U(1)_Y$ | 1/6 | -1/3 | +2/3 | -1/2 | -1 | 1/2 | 1/2 | 0 | 0 |
| $U(1)_{B-L}$ | 1/3 | 1/3 | 1/3 | -1 | -1 | 0 | 0 | +2 | -1 |
| Z_2 | + | + | + | + | + | + | - | + | - |

TABLE I: The charge assignment of fields.

model with gauged $B-L$ symmetry proposed by us [24]. We find parameter values consistent with experiments by taking into account the neutrino mass, the Higgs mass as well as the new boson mass. Then, we predict the spin-independent cross section consistent with the dark matter abundance. Various radiative seesaw mechanism with Z_2 parity and gauged $U(1)_{B-L}$ symmetries have been proposed [24–36]. Our following discussion and results would be applicable once one tries to address the Atomki anomalies in such a model, because the required cross section and the mass determine the scale of the $U(1)_{B-L}$ symmetry.

The rest of this paper is organized as follows. In section II, we explain our model including brief review of neutrino masses. We show the interaction Lagrangian of the gauge boson with SM fermions as well as constraints for the Atomki anomalies to be explained. Then, parameters and masses consistent with experimental constraints are derived in section III. In section IV, the spin-independent cross section is predicted for the parameter values derived in section III. We summarize our study in section V.

II. MODEL

We explain our model proposed in Ref. [24]. The SM is extended by imposing the gauged $U(1)_{B-L}$ symmetry and a Z_2 parity, and also introducing two scalar particles and three right-handed neutrinos, N_R . One of the scalar particles, S , is a SM singlet and responsible for $B-L$ symmetry breaking. The other one, η , has the same quantum charge as the SM Higgs Φ and is related with the generation of neutrino masses. The scalar η and the RH neutrinos N_R are Z_2 odd while other particles are Z_2 even. The charge assignment of the particles is summarized in Table I. Here, Q^i , d_R^i , u_R^i and L^i , e_R^i are the left-handed (LH) and the right-handed quarks and leptons, respectively. Latin and Greek indices denote generation and flavor of fermions.

First, we briefly review the neutrino mass in our model. The interaction Lagrangian for the generation of neutrino mass is given by

$$\mathcal{L}_{\text{int}} = \mathcal{L}_N - V(\Phi, \eta, S), \quad (1)$$

where the Yukawa interactions are given by

$$\mathcal{L}_N = g_{i\alpha} \bar{L}^i \tilde{\eta} N_R^\alpha - \frac{Y_R^\alpha}{2} S \overline{(N_R^\alpha)^c} N_R^\alpha + h.c., \quad (2)$$

and the scalar potential is given by

$$\begin{aligned} V(\Phi, \eta, S) = & \mu_1^2 |\Phi|^2 + \mu_2^2 |\eta|^2 + \mu_S^2 |S|^2 + \lambda_1 |\Phi|^4 + \lambda_2 |\eta|^4 + \lambda_3 |\Phi|^2 |\eta|^2 + \lambda_4 |\Phi^\dagger \eta|^2 \\ & + \frac{\lambda_5}{2} [(\Phi^\dagger \eta)^2 + \text{h.c.}] + \lambda_S |S|^4 + \tilde{\lambda} |\Phi|^2 |S|^2 + \lambda |\eta|^2 |S|^2, \end{aligned} \quad (3)$$

with $\tilde{\eta} = i\sigma_2 \eta^*$. The summation over repeated indices should be understood. Because of the Z_2 parity, neutrinos can not have Yukawa couplings with the Higgs field Φ ; instead, they can have those with η . After the Higgs and the scalar S develop vacuum expectation values (VEVs),

$$\langle \Phi \rangle = \frac{1}{\sqrt{2}} \begin{pmatrix} 0 \\ v \end{pmatrix}, \quad \langle S \rangle = \frac{v_S}{\sqrt{2}}, \quad (4)$$

where $v = 246$ GeV, the masses of neutrinos are generated via a one-loop diagram in which N_R and η propagate, and expressed as

$$m_{\nu L}^{ij} \simeq \frac{\lambda_5}{8\pi^2} g_{i\alpha} Y_R^\alpha g_{\alpha j}^T \left(\frac{v}{m_\eta} \right)^2 v_S. \quad (5)$$

More details can be found in Ref. [24].

Next, we consider the gauge sector. The relevant Lagrangian to explain the Atomki anomalies is given by

$$\mathcal{L} = \mathcal{L}_{\text{gauge,int}} + \mathcal{L}_{\text{gauge,kin}}, \quad (6)$$

where

$$\mathcal{L}_{\text{gauge,int}} = g_1 \hat{B}_\mu J_1^\mu + g_2 \hat{W}_\mu^a J_2^{a\mu} + \epsilon_X e \hat{X}_\mu J_X^\mu, \quad (7a)$$

$$\mathcal{L}_{\text{gauge,kin}} = -\frac{1}{4} \hat{B}_{\mu\nu} \hat{B}^{\mu\nu} - \frac{1}{4} \hat{W}_{\mu\nu}^a \hat{W}^{a\mu\nu} - \frac{1}{4} \hat{X}_{\mu\nu} \hat{X}^{\mu\nu} + \frac{\epsilon}{2} \hat{B}_{\mu\nu} \hat{X}^{\mu\nu}. \quad (7b)$$

Here, \hat{B} , \hat{W}^a , \hat{X} represent $U(1)_Y$, $SU(2)_W$ and $U(1)_{B-L}$ gauge bosons in the interaction basis, in which a being $SU(2)$ index, while $\hat{B}^{\mu\nu}$, $\hat{W}^{a\mu\nu}$, $\hat{X}^{\mu\nu}$ are their field strengths, respectively. The coupling constants and the currents of $U(1)_Y$, $SU(2)_W$ and $U(1)_{B-L}$ are denoted as g_1 , g_2 and $\epsilon_X e$, and J_1^μ , $J_2^{a\mu}$ and

$$J_X^\mu = \frac{1}{3} \bar{u}^i \gamma^\mu u^i + \frac{1}{3} \bar{d}^i \gamma^\mu d^i - \bar{e}^i \gamma^\mu e^i - \bar{\nu}^i \gamma^\mu \nu^i - \bar{N}_R^i \gamma^\mu N_R^i. \quad (8)$$

Note that the gauge coupling constant of $U(1)_{B-L}$ is normalized by the electric charge of electron for convenience. The kinetic mixing parameter is denoted as ϵ .

After the electroweak and the $B - L$ symmetries are broken, the interaction Lagrangian of the neutral gauge bosons in the mass basis is given as

$$\begin{aligned} \mathcal{L}_{\text{gauge,int}} = & eA_\mu J_{em}^\mu + Z_\mu \left[g_2(c_\chi - \varepsilon s_W s_\chi) J_{NC}^\mu + \varepsilon c_W s_\chi J_{em}^\mu + \varepsilon_X e s_\chi J_X^\mu \right] \\ & + X_\mu \left[\varepsilon_X e c_\chi J_X^\mu + \varepsilon e c_W c_\chi J_{em}^\mu - g_2(s_\chi + \varepsilon s_W c_\chi) J_{NC}^\mu \right], \end{aligned} \quad (9a)$$

$$\mathcal{L}_{\text{gauge,kin}} = -\frac{1}{4} F_{\mu\nu} F^{\mu\nu} - \frac{1}{4} Z_{\mu\nu} Z^{\mu\nu} + \frac{1}{2} m_Z^2 Z_\mu Z^\mu - \frac{1}{4} X_{\mu\nu} X^{\mu\nu} + \frac{1}{2} m_X^2 X_\mu X^\mu, \quad (9b)$$

where $A_\mu(F_{\mu\nu})$ and $Z_\mu(Z_{\mu\nu})$ represent the SM photon and the Z boson (and their field strengths), respectively. The currents J_{em}^μ and J_{NC}^μ are the same as those in the SM. The dimensionless parameters ε and ε_X are defined as

$$\varepsilon = \varepsilon r, \quad \varepsilon_X = \varepsilon_X r, \quad (10)$$

with $r = (1 - \varepsilon^2)^{-1/2}$. The weak mixing angle is denoted as $s_W = \sin \theta_W$ ($c_W = \cos \theta_W$), and the mixing angle of the gauge bosons due to the kinetic mixing, $s_\chi = \sin \chi$ ($c_\chi = \cos \chi$), is defined by

$$\tan 2\chi = \frac{-m_Z^2 q}{(1 - q^2)m_Z^2 - m_X^2 r^2}, \quad (11)$$

with $q = -\varepsilon s_W$, and

$$m_{\hat{Z}} = \frac{1}{2} \sqrt{g_1^2 + g_2^2} v, \quad (12a)$$

$$m_{\hat{X}} = 2\varepsilon_X e v s. \quad (12b)$$

The masses of the gauge bosons are given as

$$m_Z^2 = \frac{1}{2} \left[m_{\hat{Z}}^2(1 + q^2) + m_{\hat{X}}^2 r^2 + \sqrt{D} \right], \quad (13a)$$

$$m_X^2 = \frac{1}{2} \left[m_{\hat{Z}}^2(1 + q^2) - m_{\hat{X}}^2 r^2 + \sqrt{D} \right], \quad (13b)$$

$$D = (m_{\hat{Z}}^2(1 + q^2) + m_{\hat{X}}^2 r^2)^2 - 4m_{\hat{Z}}^2 m_{\hat{X}}^2 r^2. \quad (13c)$$

For $|\varepsilon|, |\varepsilon_X| \ll 1$, the mixing angle can be approximated

$$s_\chi \simeq -\varepsilon s_W, \quad c_\chi \simeq 1. \quad (14)$$

Then, the interaction Lagrangian and the gauge boson masses are given by

$$\mathcal{L}_{\text{gauge,int}} = eA_\mu J_{em}^\mu + g_2 Z_\mu J_{NC}^\mu + eX_\mu \left[\varepsilon_X J_X^\mu + \varepsilon c_W J_{em}^\mu \right] + \mathcal{O}(\varepsilon^2, \varepsilon \varepsilon_X), \quad (15a)$$

$$m_Z^2 \simeq m_{\hat{Z}}^2 + \mathcal{O}(\varepsilon^2), \quad (15b)$$

$$m_X^2 \simeq m_{\hat{X}}^2 + \mathcal{O}(\varepsilon^2). \quad (15c)$$

From Eq. (15a), the resulting coupling constants of the SM fermions to the X boson are

$$\varepsilon_u = \frac{1}{3}\varepsilon_X + \frac{2}{3}\varepsilon_{c_W}, \quad (16a)$$

$$\varepsilon_d = \frac{1}{3}\varepsilon_X - \frac{1}{3}\varepsilon_{c_W}, \quad (16b)$$

$$\varepsilon_\nu = -\varepsilon_X, \quad (16c)$$

$$\varepsilon_e = -\varepsilon_X - \varepsilon_{c_W}. \quad (16d)$$

The coupling constants of an up and a down quark can be translated into those of a proton and a neutron as

$$\varepsilon_p = 2\varepsilon_u + \varepsilon_d, \quad \varepsilon_n = \varepsilon_u + 2\varepsilon_d. \quad (17)$$

To explain the Atomki anomalies, $|\varepsilon_n|$ and $|\varepsilon_p|$ are required to satisfy [16]

$$|\varepsilon_n| = (2 - 10) \times 10^{-3}, \quad (18a)$$

$$|\varepsilon_p| \lesssim 1.2 \times 10^{-3}. \quad (18b)$$

On the other hand, these coupling constants are constrained by several experiments, i.e. the dark photon searches in neutral pion decays, beam dump searches, neutrino-electron scatterings. The constraints as well as the signal requirements are summarized as [16]

$$|\varepsilon_n| = |\varepsilon_X| = (2 - 10) \times 10^{-3}, \quad (19a)$$

$$|\varepsilon_p| = |\varepsilon_X - \varepsilon_{c_W}| \lesssim 1.2 \times 10^{-3} \quad (19b)$$

$$|\varepsilon_e| = (0.2 - 1.4) \times 10^{-3} \quad (19c)$$

$$\sqrt{|\varepsilon_e \varepsilon_\nu|} \lesssim 3 \times 10^{-4}. \quad (19d)$$

Note that in our model, $\varepsilon_\nu = -\varepsilon_n$ and hence the above experimental constraints are not satisfied. However, it is possible to evade the constraint by further extensions. One of such successful extensions is to introduce pairs of vectorlike leptons [16] whose SM gauge charges are the same while the $B - L$ charge is opposite. Because of the opposite $B - L$ charge, the mixing between the LH neutrinos and the vectorlike neutrinos can suppress the lightest neutrino coupling to X so that the constraints can be satisfied. This extension can be applied to our model and make the lightest neutrino to be neutralized to the X boson. For concreteness, we consider one pair of the vectorlike leptons $L_L^4 = (\nu_L^4, e_L^4)^T$, $L_R^4 = (\nu_R^4, e_R^4)^T$ and E_L^4 , E_R^4 that are $SU(2)_W$ doublet and singlet, respectively. We assign the even parity of Z_2 to these leptons. Then, the mass term of the neutrinos after the symmetry breaking is given by

$$\mathcal{L}_{\text{mass}} = -\frac{1}{2}m_M \overline{N_R^c} N_R - M_{4L} \overline{\nu_R^4} \nu_L - M_L \overline{\nu_L^4} \nu_R^4 + h.c., \quad (20)$$

where m_M and M_{4L} are proportional to v_S , and M_L is a Dirac mass. It is important to note that the RH neutrinos can not mix with the other neutrinos due to the Z_2 parity and hence,

be taken as mass eigenstates. The second and the third terms of Eq.(20) can be casted as $\overline{\psi}_L^\nu M_\nu \psi_R^\nu + h.c.$ where

$$M_\nu = \begin{pmatrix} 0 & M_{4L} \\ 0 & M_L \end{pmatrix}, \quad (21a)$$

$$\psi_L^\nu = \begin{pmatrix} \nu_L \\ \nu_L^4 \end{pmatrix}, \quad (21b)$$

$$\psi_R^\nu = \begin{pmatrix} N_R \\ \nu_R^4 \end{pmatrix}. \quad (21c)$$

Diagonalizing Eq.(21a), we obtain the one Dirac state with mass $\sqrt{M_L^2 + M_{4L}^2}$ and one massless state. The latter state can be express as

$$\frac{1}{\sqrt{M_L^2 + M_{4L}^2}}(-M_L \nu + M_{4L} \nu_L^4), \quad (22)$$

and its coupling to the X boson is given by

$$\epsilon_\nu = -\epsilon_X \cos 2\theta_\nu, \quad (23)$$

where $\tan \theta_\nu = M_{4L}/M_L$. Thus the lightest neutrino can be neutralized by choosing $M_{4L} \simeq M_L$. Generalization of N pairs of the vectorlike leptons is straightforward and that allows new vector lepton to be heavier while the lightest neutrino is kept neutralized.

III. PARAMETER VALUES

In this section, we show parameter values in the model taking into account the X gauge boson mass and couplings.

Firstly, the VEV of S can be determined since the mass of the gauge boson (15c) should be $m_X = 16.70 \pm 0.35(\text{stat}) \pm 0.5(\text{syst})$ MeV [14],

$$v_s = 13.78 \left(\frac{2 \times 10^{-3}}{|\epsilon_X|} \right) \text{ GeV}, \quad (24)$$

for the central value of m_X . We normalize $|\epsilon_X|$ by 2×10^{-3} as a reference value, which corresponds to the lower bound in Eq. (19a). On the other hand, the Higgs mass is given roughly by $\sqrt{2\lambda_1}v$ where λ_1 is the quartic coupling in Eq. (3). Therefore, the quartic coupling λ_1 must be 0.130 to reproduce the Higgs mass 125 GeV. Using Eq. (24), the ratio of the VEVs, $\tan \beta$, and the mixing angle between Z_2 even scalars, α , defined in Ref. [24] are expressed as

$$\tan \beta = 5.60 \times 10^{-2} \left(\frac{2 \times 10^{-3}}{|\epsilon_X|} \right), \quad (25a)$$

$$\alpha \simeq 10^{-4} \left(\frac{\tilde{\lambda}}{4.65 \times 10^{-4}} \right) \left(\frac{0.130}{\lambda_1} \right) \left(\frac{2 \times 10^{-3}}{|\epsilon_X|} \right), \quad (25b)$$

where $\tilde{\lambda}$ and λ_1 are normalized by reference values, respectively.

Then, the masses of the Z_2 even lighter scalar H and N_R are parametrized by

$$m_H = 19.5 \left(\frac{\lambda_s}{1} \right)^{1/2} \left(\frac{2 \times 10^{-3}}{|\varepsilon_X|} \right) \text{ GeV}, \quad (26a)$$

$$m_{N_R} = 9.75 \left(\frac{Y_R}{1} \right) \left(\frac{2 \times 10^{-3}}{|\varepsilon_X|} \right) \text{ GeV}, \quad (26b)$$

where λ_s and Y_R is a quartic coupling in the scalar potential and the couplings of RH neutrinos to S , respectively. One can see from Eqs. (26) that the masses of H and N_R are less than 20 and 10 GeV, respectively, when we require $\lambda_s, Y_R \leq 1$. These mass ranges are a direct consequence of the light gauge boson because the masses are proportional to v_S . Since the other Z_2 odd particle, η , should be heavier than TeV to give tiny neutrino masses, the lightest RH neutrino is the DM candidate in our model.

In the end, the LH neutrino masses given in Eq. (5) are parametrized as

$$m_{\nu_L} \sim 0.10 \left(\frac{\lambda_5 g_{i\alpha}^2}{5.7 \times 10^{-9}} \right) \left(\frac{Y_R}{1} \right) \left(\frac{v/m_\eta}{0.1} \right) \left(\frac{2 \times 10^{-3}}{|\varepsilon_X|} \right) \text{ eV}. \quad (27)$$

Adjusting λ_5 and $g_{i\alpha}$, the LH neutrino masses can be taken to the correct order, 0.1 eV, without conflicting other constraints. As shown in the next section, direct detection searches of the DM constrains α to be as small as $\mathcal{O}(10^{-4})$, and hence $\tilde{\lambda}$ should be smaller than $\mathcal{O}(10^{-4})$. This fact implies that H and N_R almost decouple from the SM sector because H consists mainly of S . The SM Higgs boson h can decay into a pair of three light particles. However, the decay widths of h into HH , $N_R N_R$, and XX pairs are

$$\Gamma(h \rightarrow N_R N_R) = 6.21 \times 10^{-7} \text{ MeV}, \quad (28a)$$

$$\Gamma(h \rightarrow HH) = 1.03 \times 10^{-3} \text{ MeV}, \quad (28b)$$

$$\Gamma(h \rightarrow XX) = 1.02 \times 10^{-3} \text{ MeV}, \quad (28c)$$

for the above reference values. Therefore the contribution to the invisible Higgs decay width is negligible.

IV. DARK MATTER

The thermal relic abundance of the lightest right-handed neutrino N_R dark matter is obtained by integrating the Boltzmann equation for its number density n ,

$$\frac{dn}{dt} + 3 \left(\frac{\dot{a}(t)}{a(t)} \right) n = -\langle \sigma v \rangle (n^2 - n_{\text{EQ}}^2), \quad (29)$$

where $a(t)$ is the scale factor of the expanding Universe, the dot denotes the derivative with respect to time, $\langle \sigma v \rangle$ is the thermal averaged annihilation cross section times relative velocity, and n_{EQ} is the dark matter number density in thermal equilibrium, respectively.

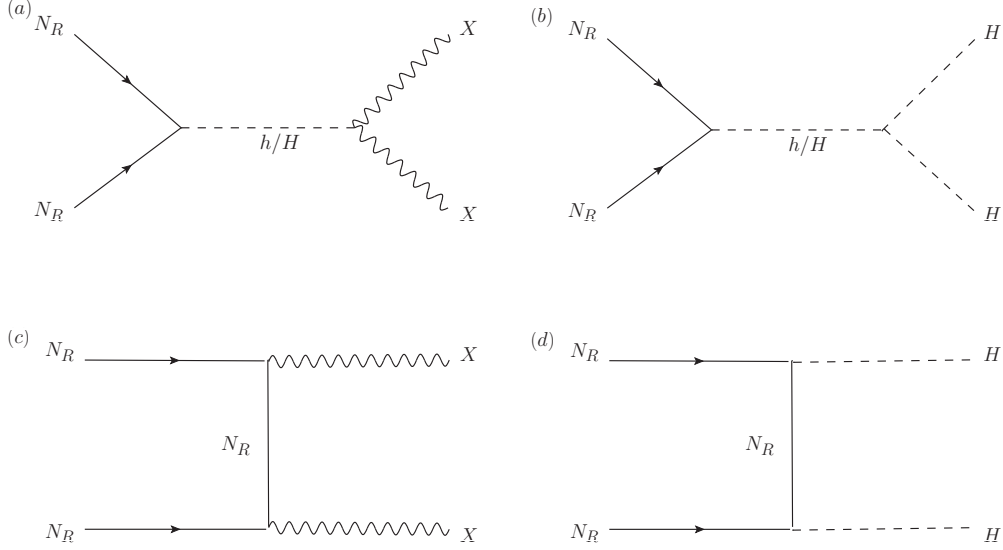


FIG. 1: The RH neutrino annihilation channels into XX and HH .

The lightest RH neutrino dominantly annihilates into pairs of the X boson and the second Higgs boson H via s-channels H exchange shown in Fig. 1(a) and 1(b). Annihilation cross section into X and H bosons pair through t-(u-) channels of the N_R exchange in Fig. 1(c) and 1(d) is 10^5 times smaller than that of the s-channel H exchange and hence, negligible. Other annihilation modes into the SM fermions through the s-channel exchange of the Higgs bosons (h and H) and the X gauge boson [37] are less important, we have included those modes in our numerical calculation nevertheless. We note formula for those annihilation modes in the Appendix for information. The dominant annihilation mode is $N_R N_R \rightarrow XX$ for a large parameter region. With suggested couplings constant values shown in Eq. (19a), we obtain

$$m_{DM} \simeq 3.4 \text{ GeV}, \quad (30)$$

in a heavy H cases ($m_H \gtrsim 9 \text{ GeV}$) and which is the maximum dark matter mass in our model. Figure 2 shows the thermal relic abundance of the lightest right-handed neutrino $\Omega_{N_R} h^2$ in terms of m_{N_R} . The orange line indicates $\Omega_{DM} h^2 \simeq 0.12$ as measured by the Planck satellite [38]. The blue and green curves are for $m_H = 9 \text{ GeV}$ and 2 GeV , respectively, as reference values. For light m_H , lighter DM mass regions also become viable due to features depend on m_H . Although typical dark matter abundance is large for $m_{DM} < 3.4 \text{ GeV}$, even in such a region, the relic abundance is significantly reduced by the resonant annihilation for $m_{N_R} = m_H/2$ and can meet with its observed value. This annihilation appears as the deep and narrow gaps in the abundance, which can be seen in the figure. The other characteristic appears at the $m_{N_R} = m_H$ where the annihilation channel into a HH pair is kinematically open, and it dominates the annihilation cross section. The sudden decrease of the relic abundance on the left side is explained by this mode.

Thus, one can understand from the figure that the dark matter abundance can be repro-

duced for the two cases of m_{N_R} : (1) at just below the threshold of the H pair annihilation and (2) at both sides of the H resonance or at the off resonance. In the former case, the dark matter mass is determined by

$$m_{DM} \simeq m_H. \quad (31)$$

In the Fig. 2, the dark matter mass is obtained as

$$m_{DM} = 2 \text{ GeV}, \quad (32)$$

for $m_H = 2 \text{ GeV}$. As m_{N_R} as well as m_H are heavy, the annihilation cross section becomes larger and hence the dark matter abundance can not be explained for $m_H = 9 \text{ GeV}$. In the latter case, the dark matter mass is given by

$$m_{DM}^{\pm} = \frac{m_H}{2} \pm \delta m, \quad (33)$$

where the mass difference δm is typically from 0.5 GeV ($m_H = 2 \text{ GeV}$) to 1 GeV ($m_H = 9 \text{ GeV}$). For $m_H = 9 \text{ GeV}$, the dark matter mass is determined as

$$m_{DM}^- \sim 3.4 \text{ GeV}, \quad (34)$$

while for $m_H = 2 \text{ GeV}$,

$$m_{DM}^{\pm} = 0.5 \text{ or } 1.5 \text{ GeV}. \quad (35)$$

We note that the results are independent from $\sin \alpha$ as its main annihilation mode are. One may notice that those annihilation processes have a tiny s-wave component and are dominantly p-wave.

This N_R dark matter can be searched through the elastic scattering off with a nucleon. The spin-independent scattering cross section with a proton through Higgs bosons exchange is given by [39]

$$\sigma^{\text{SI}} = \frac{4}{\pi} \left(\frac{m_p m_{N_R}}{m_p + m_{N_R}} \right)^2 f_p^2, \quad (36)$$

with the proton mass m_p and the effective spin-independent coupling between N_R and a proton, f_p , which is given as

$$\frac{f_p}{m_p} = \sum_{q=u,d,s} f_{Tq}^{(p)} \frac{\alpha_q}{m_q} + \frac{2}{27} f_{TG}^{(p)} \sum_{c,b,t} \frac{\alpha_q}{m_q}, \quad (37)$$

where m_q is a quark mass, $f_{Tq}^{(p)}$ and $f_{TG}^{(p)}$ are constants. The effective vertices between N_R and a quark also have been derived in Ref. [37] as

$$\alpha_q = -\frac{m_{N_R} m_q}{v_s v} \sin \alpha \cos \alpha \left(\frac{1}{m_h^2} - \frac{1}{m_H^2} \right). \quad (38)$$

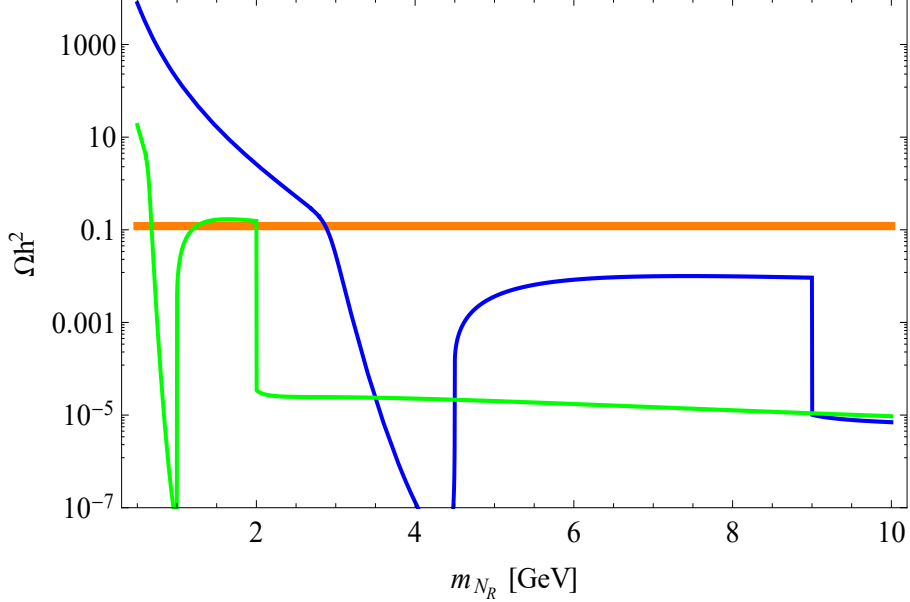


FIG. 2: The right-handed neutrino dark matter thermal relic abundance. The blue and green lines are for $m_H = 9$ GeV and 2 GeV, respectively. The orange line indicates $\Omega_{DM}h^2 \simeq 0.12$ as measured by Planck satellite.

Figure 3 displays the prediction of σ^{SI} . We have searched points satisfying $\Omega_{N_R}h^2 \simeq 0.1$ by varying the masses of dark matter m_{N_R} and mediator m_H . The red (blue) points show the results for $\sin \alpha = 1 \times 10^{-4}$ (1×10^{-5}). Here we have scanned m_H for $2 \text{ GeV} \leq m_H \leq 10 \text{ GeV}$, which is enough to find mass range of dark matter. The lower bound on m_H we took is due to the following reason. The radiative correction to λ_s from one loop diagram propagating N_R is $\delta\lambda_s \simeq -(1/4\pi^2) \sum Y_R^4$. Provided that the largest coupling of Y_R is the order of unity, as we often think from the viewpoint of “naturalness”, then we have $\delta\lambda_s = \mathcal{O}(-0.01)$. Thus, by considering such radiative corrections, $\lambda_s = 0.01$ seems to be a sensible lower value and its corresponding Higgs boson mass estimated from Eq. (26a) is about 2 GeV. We show excluded regions by direct dark matter searches, the CREEST-II [40], the CDMSlite [41] and the LUX [42, 43]. For both red and blue points, one can see two groups of points; the upper group predicting a larger cross section with a nucleon and the lower group predicting a smaller cross section. The former corresponds to the case of Eq. (31) and m_{DM}^+ in Eq.(33) and the later does to the case of Eq. (34) and m_{DM}^- in Eq.(33). The projected sensitivity of the SuperCDMS SNOLAB [44] can cover the predicted regions of $\sin \alpha > \mathcal{O}(10^{-5})$.

As we mentioned above, among the dominant annihilation into X bosons pair, only t-(u-) channel N_R exchange contribution gives a small s-wave mode of $\mathcal{O}(10^{-5})$ pb. Hence, the bounds from dark matter indirect searches such as the Fermi-LAT [45] do not constrain a parameter region of interest in this model. It has been pointed out that, in light of AMS-02 data [46], a low mass region ($m_{DM} < \mathcal{O}(0.1)$ GeV) of dark matter annihilating into electrons

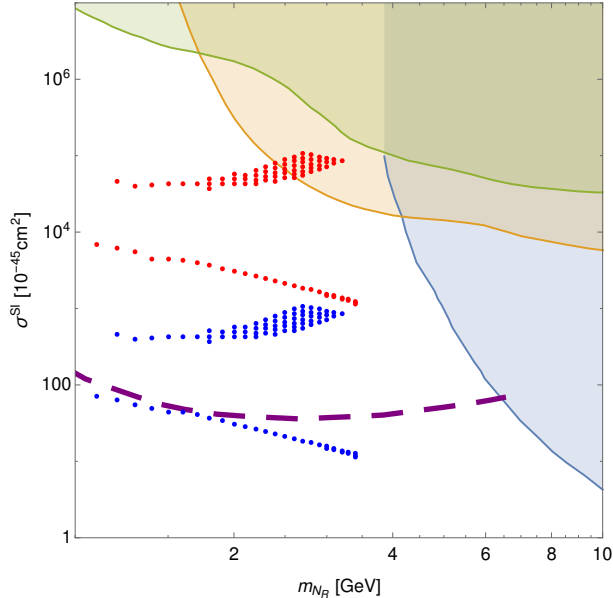


FIG. 3: The spin-independent scattering cross section with a proton. The red (blue) points are for $\sin \alpha = 1 \times 10^{-4}$ (1×10^{-5}). The excluded regions by null results in the CREEST-II, the CDMSlite and the LUX have shading with green, orange and blue, respectively. The purple dashed line indicates the expected sensitivity of Ge HV detector in the superCDMS SNOWLAB

is stringently constrained [47]. Even with such a small annihilation cross section, it is not trivial to confirm that this constraint is satisfied for a light mass region. Thus, we restrict investigated dark matter mass range at GeV region in this paper, we might study such light region elsewhere.

V. SUMMARY

Motivated by the Atomki anomalies and nonvanishing neutrino masses, we have considered a gauged $U(1)_{B-L}$ extended radiative seesaw model. We showed that the anomalies as well as the dark matter abundance and nonvanishing neutrino masses can be explained simultaneously.

Requiring the decay of the $B - L$ gauge boson to be the origin of the Atomki anomalies, we showed that the model parameters can be determined or constrained. The resulting mass of the lightest right-handed neutrino dark matter is below about 3.4 GeV and that of the lighter Z_2 even scalar is also below about 20 GeV assuming the coupling to be smaller than the unity. However, such light particles must almost decouple from the SM due to small couplings. Therefore, the Higgs sector remains the SM-like, which is consistent with the LHC results.

We have also found that the relic dark matter abundance can be reproduced by the

annihilation into XX . It further constrains the scalar mixing angle and the dark matter mass. We have shown the consistent model parameter region with $\Omega_{N_R} h^2 \simeq 0.1$ where the elastic scattering cross section of the DM particle off nuclei can be below the current bound from the CRESST-II, the CDMSlite and LUX experiments. However, the cross section is predicted within the reach of the expected sensitivity of Ge HV detector. Therefore, our dark matter candidate is in practice detectable even for an extremely small Higgs mixing angle $\sin \alpha$.

Acknowledgments

T. S would like to thank Y. Maeda for fruitful discussion on nuclear experiments. We are grateful for M. Aoki's valuable comments letting us notice an error in the previous calculation. This work is supported, in part, by JSPS KAKENHI Grants No. 15K17654 (T. S) and No. 26400243 (O. S.) and by the SUHARA Memorial Foundation (O. S.).

Appendix A: Amplitude

We give explicit formulas of the invariant amplitude squared for the pair annihilation processes of the RH neutrinos.

1. Annihilation into XX

\mathcal{M}_1 denotes the amplitude by the s -channel Higgs bosons h and H exchange, while \mathcal{M}_2 does that for the $t(u)$ -channel N exchange diagram.

$$|\overline{\mathcal{M}}|^2 = |\overline{\mathcal{M}_1 + \mathcal{M}_2}|^2, \quad (\text{A1})$$

$$|\overline{\mathcal{M}_1}|^2 = m_N^2 q_{B-L}^2 g_{B-L}^2 \left| \sin^2 \alpha \frac{1}{s - m_h^2 + im_h \Gamma_h} + \cos^2 \alpha \frac{1}{s - m_H^2 + im_H \Gamma_H} \right|^2$$

$$\times (s - 4m_N^2) \left(1 + \frac{1}{2m_X^4} \left(\frac{s}{2} - m_X^2 \right)^2 \right), \quad (\text{A2})$$

$$\int \frac{d \cos \theta}{2} |\overline{\mathcal{M}_2}|^2 = \frac{32g_{B-L}^4 q_{B-L}^4}{m_X^4}$$

$$\left(\frac{4m_N^4 s (s - 4m_X^2) + 4m_N^2 m_X^2 (4m_X^2 - s) (m_X^2 + s) - m_X^4 (4m_X^4 + s^2)}{\sqrt{s - 4m_N^2} \sqrt{s - 4m_X^2} (s - 2m_X^2)} \right.$$

$$\times \ln \left[\frac{s - 2m_X^2 - \sqrt{s - 4m_N^2} \sqrt{s - 4m_X^2}}{s - 2m_X^2 + \sqrt{s - 4m_N^2} \sqrt{s - 4m_X^2}} \right]$$

$$\left. + \frac{2m_N^4 (8m_X^4 - 8m_X^2 s + s^2) + m_N^2 m_X^4 (4m_X^2 + s) - 2m_X^8}{(m_N^2 (s - 4m_X^2) + m_X^4)} \right), \quad (\text{A3})$$

$$\int \frac{d \cos \theta}{2} (\overline{\mathcal{M}_1 \mathcal{M}_2^* + c.c.})$$

$$= \frac{8\sqrt{2}g_{B-L}^4 q_{B-L}^4 v_s \lambda m_N}{m_X^4 \sqrt{s - 4m_N^2} \sqrt{s - 4m_X^2}} \left(\frac{-\sin \alpha (m_h^2 - s)}{\Gamma_h^2 m_h^2 + (m_h^2 - s)^2} + \frac{\cos \alpha (m_H^2 - s)}{\Gamma_H^2 m_H^2 + (m_H^2 - s)^2} \right)$$

$$\times \left(\sqrt{s - 4m_N^2} (4m_X^4 - 2m_X^2 s + s^2) \sqrt{s - 4m_X^2} \right.$$

$$\left. + 2(m_N^2 (8m_X^4 - 4m_X^2 s + s^2) - 2m_X^6) \log \left[\frac{s - 2m_X^2 - \sqrt{s - 4m_N^2} \sqrt{s - 4m_X^2}}{s - 2m_X^2 + \sqrt{s - 4m_N^2} \sqrt{s - 4m_X^2}} \right] \right), \quad (\text{A4})$$

where θ is the scattering angle in the center of mass frame.

2. Annihilation into HH

\mathcal{M}_1 denotes the amplitude by the s -channel Higgs bosons h and H exchange, while \mathcal{M}_2 does that for the $t(u)$ -channel N exchange diagram.

$$|\overline{\mathcal{M}}|^2 = |\overline{\mathcal{M}_1 + \mathcal{M}_2}|^2, \quad (\text{A5})$$

$$|\overline{\mathcal{M}_1}|^2 = \frac{\lambda_N^2}{4}(s - 4m_N^2) \left| \frac{\sin \alpha}{s - m_h^2 + im_h \Gamma_h} \lambda_{hHH} - \frac{\cos \alpha}{s - m_H^2 + im_H \Gamma_H} \lambda_{HHH} \right|^2, \quad (\text{A6})$$

$$\begin{aligned} & \int \frac{d \cos \theta}{2} |\overline{\mathcal{M}_2}|^2 \\ = & \frac{\lambda_N^4}{2} \cos^4 \alpha \left(-8 - \frac{4(m_H^2 - 4m_N^2)^2}{m_H^4 - 4m_H^2 m_N^2 + m_N^2 s} + \right. \\ & \left. 4 \frac{(6m_H^4 - 32m_N^4 + 16m_N^2 s + s^2 - 4m_H^2(4m_N^2 + s))}{(s - 2m_H^2)\sqrt{(s - 4m_N^2)(s - 4m_H^2)}} \ln \left[\frac{s - 2m_H^2 + \sqrt{(s - 4m_N^2)(s - 4m_H^2)}}{s - 2m_H^2 - \sqrt{(s - 4m_N^2)(s - 4m_H^2)}} \right] \right), \end{aligned} \quad (\text{A7})$$

$$\begin{aligned} & \int \frac{d \cos \theta}{2} (\overline{\mathcal{M}_1 \mathcal{M}_2^* + c.c}) \\ = & 8\sqrt{2} \lambda_N^3 m_N \cos^2 \alpha \left(-\frac{\sin \alpha (s - m_h^2) \lambda_{hHH}}{(s - m_h^2)^2 + (M_h \Gamma_h)^2} + \frac{\cos \alpha (s - m_H^2) \lambda_{HHH}}{(s - m_H^2)^2 + (M_H \Gamma_H)^2} \right) \\ & \left(1 + \frac{s - 8m_N^2 + 2m_H^2}{2\sqrt{(s - 4m_N^2)(s - 4m_H^2)}} \ln \left[\frac{s - 2m_H^2 + \sqrt{(s - 4m_N^2)(s - 4m_H^2)}}{s - 2m_H^2 - \sqrt{(s - 4m_N^2)(s - 4m_H^2)}} \right] \right). \end{aligned} \quad (\text{A8})$$

-
- [1] P. Minkowski, Phys. Lett. **B67**, 421 (1977).
 - [2] T. Yanagida, Conf. Proc. **C7902131**, 95 (1979).
 - [3] M. Gell-Mann, P. Ramond, and R. Slansky, Conf. Proc. **C790927**, 315 (1979), 1306.4669.
 - [4] R. N. Mohapatra and G. Senjanovic, Phys. Rev. Lett. **44**, 912 (1980).
 - [5] W. Konetschny and W. Kummer, Phys. Lett. **B70**, 433 (1977).
 - [6] T. P. Cheng and L.-F. Li, Phys. Rev. **D22**, 2860 (1980).
 - [7] J. Schechter and J. W. F. Valle, Phys. Rev. **D22**, 2227 (1980).
 - [8] R. Foot, H. Lew, X. G. He, and G. C. Joshi, Z. Phys. **C44**, 441 (1989).
 - [9] A. Zee, Phys. Lett. **B93**, 389 (1980), [Erratum: Phys. Lett. B95,461(1980)].
 - [10] A. Zee, Nucl. Phys. **B264**, 99 (1986).
 - [11] K. S. Babu, Phys. Lett. **B203**, 132 (1988).
 - [12] L. M. Krauss, S. Nasri, and M. Trodden, Phys. Rev. **D67**, 085002 (2003), hep-ph/0210389.
 - [13] E. Ma, Phys. Rev. **D73**, 077301 (2006), hep-ph/0601225.
 - [14] A. J. Krasznahorkay et al., Phys. Rev. Lett. **116**, 042501 (2016), 1504.01527.
 - [15] J. L. Feng, B. Fornal, I. Galon, S. Gardner, J. Smolinsky, T. M. P. Tait, and P. Tanedo, Phys. Rev. Lett. **117**, 071803 (2016), 1604.07411.

- [16] J. L. Feng, B. Fornal, I. Galon, S. Gardner, J. Smolinsky, T. M. P. Tait, and P. Tanedo, *Phys. Rev.* **D95**, 035017 (2017), 1608.03591.
- [17] P.-H. Gu and X.-G. He (2016), 1606.05171.
- [18] M. J. Neves and J. A. Helayel-Neto (2016), 1609.08471.
- [19] Y. Kahn, G. Krnjaic, S. Mishra-Sharma, and T. M. P. Tait (2016), 1609.09072.
- [20] U. Ellwanger and S. Moretti, *JHEP* **11**, 039 (2016), 1609.01669.
- [21] L.-B. Jia and X.-Q. Li, *Eur. Phys. J.* **C76**, 706 (2016), 1608.05443.
- [22] T. Kitahara and Y. Yamamoto, *Phys. Rev.* **D95**, 015008 (2017), 1609.01605.
- [23] C.-S. Chen, G.-L. Lin, Y.-H. Lin, and F. Xu (2016), 1609.07198.
- [24] S. Kanemura, O. Seto, and T. Shimomura, *Phys. Rev.* **D84**, 016004 (2011), 1101.5713.
- [25] T. Li and W. Chao, *Nucl. Phys.* **B843**, 396 (2011), 1004.0296.
- [26] S. Khalil, H. Okada, and T. Toma, *JHEP* **07**, 026 (2011), 1102.4249.
- [27] M. Lindner, D. Schmidt, and T. Schwetz, *Phys. Lett.* **B705**, 324 (2011), 1105.4626.
- [28] S. Kanemura, T. Nabeshima, and H. Sugiyama, *Phys. Rev.* **D85**, 033004 (2012), 1111.0599.
- [29] H. Okada and T. Toma, *Phys. Rev.* **D86**, 033011 (2012), 1207.0864.
- [30] S. Kanemura, T. Nabeshima, and H. Sugiyama, *Phys. Rev.* **D87**, 015009 (2013), 1207.7061.
- [31] Y. Kajiyama, H. Okada, and K. Yagyu, *Nucl. Phys.* **B874**, 198 (2013), 1303.3463.
- [32] Y. Kajiyama, H. Okada, and T. Toma, *Phys. Rev.* **D88**, 015029 (2013), 1303.7356.
- [33] T. Basak and T. Mondal, *Phys. Rev.* **D89**, 063527 (2014), 1308.0023.
- [34] S. Kanemura, T. Matsui, and H. Sugiyama, *Phys. Rev.* **D90**, 013001 (2014), 1405.1935.
- [35] H. Okada and Y. Orikasa, *Phys. Lett.* **B760**, 558 (2016), 1412.3616.
- [36] W. Wang and Z.-L. Han, *Phys. Rev.* **D92**, 095001 (2015), 1508.00706.
- [37] N. Okada and O. Seto, *Phys. Rev.* **D82**, 023507 (2010), 1002.2525.
- [38] P. A. R. Ade et al. (Planck), *Astron. Astrophys.* **594**, A13 (2016), 1502.01589.
- [39] G. Jungman, M. Kamionkowski, and K. Griest, *Phys. Rept.* **267**, 195 (1996), hep-ph/9506380.
- [40] G. Angloher et al. (CRESST-II), *Eur. Phys. J.* **C74**, 3184 (2014), 1407.3146.
- [41] R. Agnese et al. (SuperCDMS), *Phys. Rev. Lett.* **116**, 071301 (2016), 1509.02448.
- [42] D. S. Akerib et al. (LUX), *Phys. Rev. Lett.* **116**, 161301 (2016), 1512.03506.
- [43] D. S. Akerib et al. (LUX), *Phys. Rev. Lett.* **118**, 021303 (2017), 1608.07648.
- [44] R. Agnese et al. (2016), 1610.00006.
- [45] M. L. Ahnen et al. (Fermi-LAT, MAGIC), *JCAP* **1602**, 039 (2016), 1601.06590.
- [46] M. Aguilar et al. (AMS), *Phys. Rev. Lett.* **110**, 141102 (2013).
- [47] A. Ibarra, A. S. Lamperstorfer, and J. Silk, *Phys. Rev.* **D89**, 063539 (2014), 1309.2570.